



# Single-mismatch detection using gold-quenched fluorescent oligonucleotides

Benoit Dubertret<sup>1\*</sup>, Michel Calame<sup>1,2</sup>, and Albert J. Libchaber<sup>1</sup>

Here we describe a hybrid material composed of a single-stranded DNA (ssDNA) molecule, a 1.4 nm diameter gold nanoparticle, and a fluorophore that is highly quenched by the nanoparticle through a distance-dependent process. The fluorescence of this hybrid molecule increases by a factor of as much as several thousand as it binds to a complementary ssDNA. We show that this composite molecule is a different type of molecular beacon with a sensitivity enhanced up to 100-fold. In competitive hybridization assays, the ability to detect single-mismatch is eightfold greater with this probe than with other molecular beacons.

Hybrid materials composed of biomolecules, such as proteins or polynucleotides, and nonbiological inorganic objects (tiny particles of insulators, semiconductors, and metals) have recently been assembled<sup>1-4</sup>. The highly specific recognition properties of biomolecules combined with the unique optical properties of the inorganic nanoparticles make these composite materials attractive for use in the fields of biodiagnostics (non-photobleaching immunolabels<sup>5</sup>, sensitive probes for polynucleotide detection<sup>6-8</sup>) and nanotechnologies<sup>4</sup>. For example, gold nanocrystals may self-assemble with good spatial control of the inorganic components<sup>9,10</sup>, broadening the scope for "bottom-up" fabrication approaches. Although some fundamentally interesting properties of hybrid materials have already been discovered<sup>5,11</sup>, their use as functional materials is still very limited. Here, we introduce a hybrid material composed of a 1.4 nm diameter gold nanoparticle, an organic dye, and a 25-nucleotide-long ssDNA molecule. We show that this hybrid material can be used as a molecular beacon<sup>12</sup>, that is, a nucleic acid probe with hairpin-shaped structure in which the 5' and 3' ends are self-complementary, bringing a fluorophore and a quencher into close proximity. Fluorescence is restored when the probe binds to a complementary nucleic acid target (Fig. 1A).

Extensive study of the unique thermodynamics and specificity of molecular beacons<sup>13,14</sup> has demonstrated two main advantages: excellent sensitivity to the detection of one mismatch in a nucleic acid sequence and easy direct detection of unlabeled oligonucleotides. Although these properties have yielded new results in areas such as genomics<sup>15</sup>, DNA chips<sup>16</sup>, and quantitative PCR<sup>17,18</sup>, the great challenge still remains of improving the fluorescence quenching efficiency. The organic quencher used at present, 4-((4'-(dimethylamino)phenyl)azo)benzoic acid (DABCYL), quenches at most 99.0% of the fluorescence of the dye placed in its proximity. DABCYL optimally quenches fluorescein, but its quenching efficiency decreases for dyes emitting at longer wavelengths (see Table 2). A better quencher would greatly increase the sensitivity and the possible applications of molecular beacons.

We show that 1.4 nm diameter gold nanoparticles can advantageously replace DABCYL as a quencher of fluorescence because they quench fluorescence as much as 100 times better and have higher quenching efficiency for dyes emitting near the infrared region. The quenching properties of metal clusters have been well studied theoretically<sup>19-21</sup>, but because of the difficulties of sequentially bringing a

fluorophore and a metal cluster far apart or in close proximity, no precise measurement of the quenching efficiency of metal nanoparticles has been done so far.

The extremely high quenching efficiency reported here with gold clusters opens new perspectives in the use of hybrid materials as sensitive probes in fluorescence-based detection assays. In particular, molecular beacons with very high quenching efficiency can detect minute amounts of oligonucleotide target sequences in a pool of random sequences. Other advantages of high quenching efficiency include improved detection of a single mismatch in a competitive hybridization assay, as we show here.

## Results

**Covalent linkage of a gold nanoparticle and a fluorophore to ssDNA.** A 25-base synthetic oligonucleotide modified with a primary amine at its 3' end, and a disulfide at its 5' end, was used for all experiments reported here. The oligonucleotide can adopt a hairpin-loop structure because the five nucleotides at its extremities are complementary (Fig. 1B). The design of the sequence provides a hairpin structure that is very stable at room temperature but opens easily on hybridization of the loop to its target. First, an amine-reactive dye was coupled to the primary amine at the 3' end of the oligonucleotide. After purification, the 5'-end disulfide was cleaved and the free sulfhydryl was covalently attached to the 1.4 nm diameter gold cluster (Nanogold; Nanoprobes), which comes with one *N*-propylmaleimide and has been passivated with water-soluble phosphine ligands. The coupling was done with an excess of gold nanoparticles. We analyzed the reaction product by gel electrophoresis (Fig. 2). We also sought possible nonspecific interactions between the dye-oligonucleotide and the gold nanoparticles both on the gel and in the fluorometer. On reacting Nanogold with a dye-oligonucleotide complex missing the 5'-disulfide, we observed absolutely no quenching in the fluorometer. Furthermore, this dye-oligonucleotide mixed with gold (Fig. 2, lane R-o+G) behaves similarly to the dye-oligonucleotide conjugate (Fig. 2, lane R-o) when run on a gel. This confirms the absence of nonspecific interactions between the Nanogold and the DNA.

**Measure of the gold nanoparticle quenching efficiency.** The ssDNA molecule (Fig. 1B), conjugated at one extremity to a dye moiety and at the other to a gold nanoparticle, offers a way to test the quenching efficiency of the gold nanoparticle. The DNA can adopt two conformations (Fig. 1A): a stem-loop structure with the

<sup>1</sup>Center for Studies in Physics and Biology, The Rockefeller University, 1230 York Avenue, New York, NY 10021. <sup>2</sup>Current address: Institute of Physics, Klingelbergstrasse 82, CH-4056 Basel, Switzerland. \*Corresponding author ([benoit@pollux.rockefeller.edu](mailto:benoit@pollux.rockefeller.edu)).



## RESEARCH ARTICLE

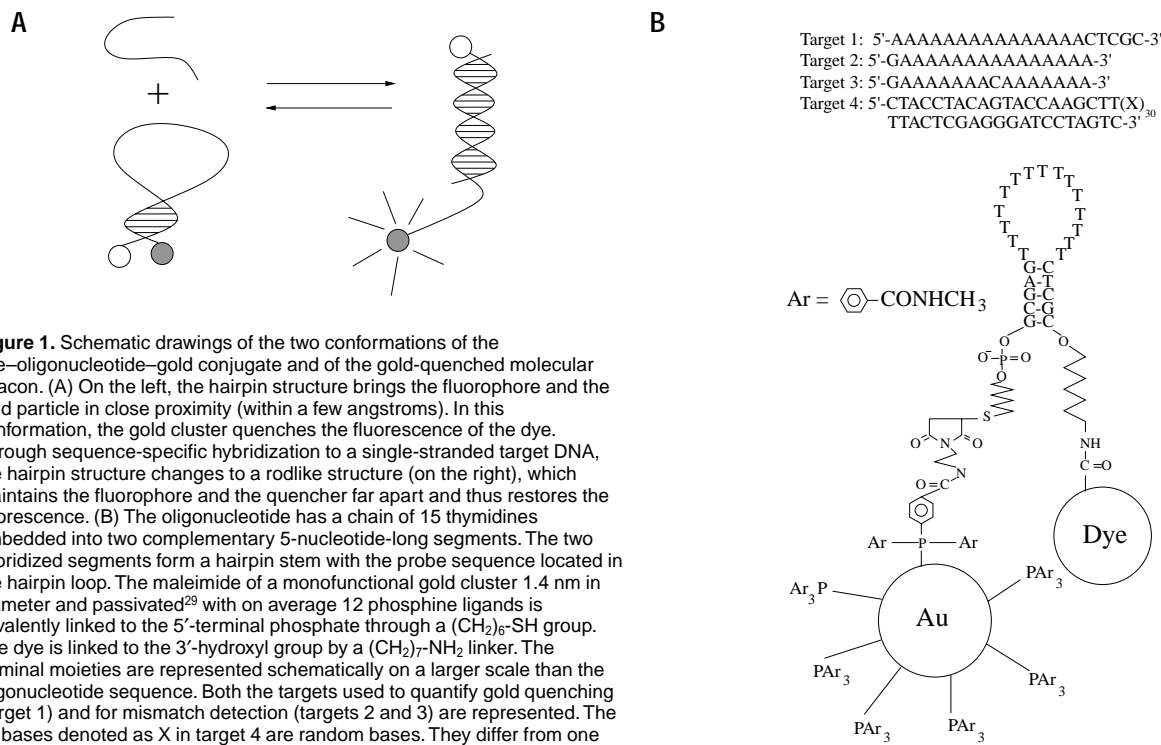


**Figure 1.** Schematic drawings of the two conformations of the dye-oligonucleotide-gold conjugate and of the gold-quenched molecular beacon. (A) On the left, the hairpin structure brings the fluorophore and the gold particle in close proximity (within a few angstroms). In this conformation, the gold cluster quenches the fluorescence of the dye. Through sequence-specific hybridization to a single-stranded target DNA, the hairpin structure changes to a rodlike structure (on the right), which maintains the fluorophore and the quencher far apart and thus restores the fluorescence. (B) The oligonucleotide has a chain of 15 thymidines embedded into two complementary 5-nucleotide-long segments. The two hybridized segments form a hairpin stem with the probe sequence located in the hairpin loop. The maleimide of a monofunctional gold cluster 1.4 nm in diameter and passivated<sup>29</sup> with on average 12 phosphine ligands is covalently linked to the 5'-terminal phosphate through a (CH<sub>2</sub>)<sub>6</sub>-SH group. The dye is linked to the 3'-hydroxyl group by a (CH<sub>2</sub>)<sub>7</sub>-NH<sub>2</sub> linker. The terminal moieties are represented schematically on a larger scale than the oligonucleotide sequence. Both the targets used to quantify gold quenching (target 1) and for mismatch detection (targets 2 and 3) are represented. The 30 bases denoted as X in target 4 are random bases. They differ from one strand of DNA to the other.

fluorophore and the gold nanoparticle held in close proximity (close state), and a rodlike structure with them far apart (open state). The quenching efficiency of the gold nanoparticle is given by  $100 \times (1 - \beta)$ , where  $\beta$  is the ratio of the fluorescence of the close to that of the open state.

All fluorescent measurements were done in a spectrofluorometer at 20°C using 3 ml cuvettes. We synthesized four different gold-oligonucleotide-dye conjugates with fluorescein, rhodamine 6G, Texas red, or cyanine-5 (Cy5). For each dye tested, the spectrofluorometer's excitation and emission wavelength was tuned to the respective maximum of excitation and emission of the dye. As shown in Figure 3, the measurements were done in three steps. First, the background fluorescence of the buffer was measured. A high concentration of salt ensures that the ssDNA forms a hairpin. Then a mix of gold nanoparticles that had been reacted in excess with oligonucleotide-dye complex (and were not purified away from beacons) was introduced in the cuvet. The fluorescence level changed slightly, depending on the quenching efficiency of the gold nanoparticle. In the last step, a single-stranded oligonucleotide complementary to the loop and to half of the stem of the hairpin DNA (Fig. 1B, target 1) was mixed in excess. As the target hybridizes to the hairpin-DNA loop, the fluorescence rises considerably.

When the mixture of gold that reacted in excess with the oligonucleotide-dye complex is introduced in the cuvet, the fluorescence intensity rises as a result of the imperfect quenching of the dye, and decreases as a result of the absorption and the scattering of part of the excitation light by the gold nanoparticles. These two competing phenomena may result in a total decrease (Fig. 3B) or increase (Fig. 3A, C, D) of collected light. The offset due to the presence of the noncoupled gold particles was measured (Table 1) by collecting the light intensity when only the gold nanoparticles are introduced in the cuvet. The ratio of the fluorescence intensity measured in the cuvet before and after adding the target gives, after compensation for the buffer's background and the offset fluorescence, the quenching efficiency of the hybrid probe (Table 1).

The best quenching efficiency is obtained when dye-oligonucleotide conjugates have been reacted with Nanogold between 12 h and two days. Longer reaction times produced probes with lower quenching efficiency. For a given dye, the measured quenching efficiency of the hybrid probe may vary strongly from one reaction to the other. The samples with the best quenching efficiencies are presented for each dye in Figure 3. The precise experimental results are reported in Table 1, as well as the average quenching efficiencies obtained for all of the coupling reactions performed for a given dye.

**Table 1. Quenching of various dyes with gold nanoparticles<sup>a</sup>**

Dye	Buffer ( $I_i$ )	Gold + probe ( $I_{ii}$ )	Gold ( $I_{iii}$ )	Gold + probe + target ( $I_{iv}$ )	QE (%)	$N_T$	$\langle QE \rangle$
Fluorescein	932 ± 1	939 ± 1	909 ± 1	6,121 ± 3	99.42 ± 0.02	4	98.68 ± 0.47
Rhodamine 6G	287.6 ± 0.8	274.7 ± 0.4	272.8 ± 1.4	5,794 ± 3	99.966 ± 0.026	13	99.45 ± 0.54
Texas red	108.8 ± 0.4	135.2 ± 0.3	93.5 ± 1.0	2,945 ± 1	98.54 ± 0.04	2	98.26 ± 0.26
Cy5	20.7 ± 0.2	31.5 ± 0.1	20.0 ± 0.2	756 ± 3	98.44 ± 0.03	3	97.5 ± 1.0

<sup>a</sup>Fluorescent intensities (in counts per second) were measured in the spectrofluorometer using a 3 ml cuvet at 20°C, from (i) the buffer alone (1 M NaCl, 10 mM cacodylic acid, 0.5 mM EDTA, pH 7.3); (ii) the mixture of gold and gold-oligonucleotide-dye conjugates in the buffer; (iii) gold alone with concentration same as in (ii); (iv) same as (ii) after the addition of an excess of perfect targets. All values are given as mean ± s.e. The values reported here correspond to the samples presented in Figure 3. The last two columns report the total number of dye-DNA-gold conjugation reactions for each dye ( $N_T$ ), and the average quenching ( $\langle QE \rangle$ ) measured for all conjugates.

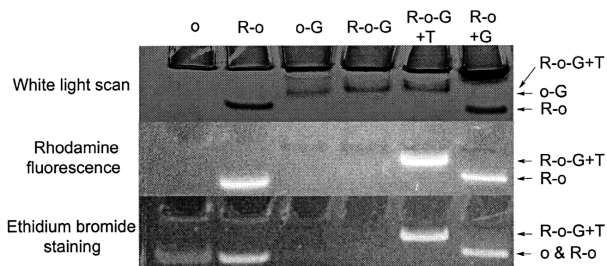


**Figure 2.** Gel electrophoresis of reaction products. From left to right: lane o, 125 pmol of nonconjugated oligonucleotide; lane R-o, 125 pmol of rhodamine 6G–oligonucleotide conjugate; lane o-G, 125 pmol of oligonucleotide reacted with 1.5 nmol of monomaleimido Nanogold; lane R-o-G, 125 pmol of rhodamine 6G–oligonucleotide conjugate reacted with 1.5 nmol of monomaleimido Nanogold; lane R-o-G+T, same as lane R-o-G with an excess of target 1 (Fig. 1B); lane R-o+G, 125 pmol of rhodamine 6G–oligonucleotide conjugate without the 5'-disulfide group reacted with 1.5 nmol of monomaleimido Nanogold. Explanation of lane labels: o, oligonucleotide; R, rhodamine 6G; G, gold nanocluster; T, target; hyphens indicate covalent bonds. The top picture is a white-light scan of the gel. Both the gold–oligonucleotide conjugates and the dye–oligonucleotide complexes are visible with the naked eye. Under UV excitation (middle picture), the dye–oligonucleotide complexes (lanes R-o, R-o-G+T, and R-o+G) produce a strong fluorescence. The dye–oligonucleotide–gold conjugates (lane R-o-G) do not emit any visible light, but the same mixture with an excess of target (lane R-o-G+T) yields a fluorescence similar in intensity to the one of the dye–oligonucleotide conjugates (lane R-o). The bare oligonucleotides (lane o) appears with ethidium bromide staining (bottom picture). Unconjugated gold nanoparticles do not penetrate the gel: they migrate in opposite direction from the DNA. Oligonucleotides missing the disulfide group do not interact with gold (lane R-o+G is similar to lane R-o).

Rhodamine 6G is the best quenched dye, with an average quenching efficiency of  $99.45 \pm 0.54\%$ . Out of 13 reactions studied, 4 produced probes with quenching efficiencies  $>99.9\%$ , and the best sample had a quenching efficiency of  $99.966 \pm 0.026\%$ . Such quenching efficiencies mean that the fluorescence intensity of a gold-quenched molecular beacon can increase by a factor of several thousand on hybridization to its perfect target.

The other dyes are not quenched as well. However, for each dye, the quenching efficiency (see Table 2) when Nanogold was used was greater than the values obtained with regular molecular beacons.

The variations in the quenching efficiency among reactions are consistent with small variations in the number of dye–oligonucleotide conjugates that are not coupled to the gold. We tried to separate the dye–oligonucleotide–gold conjugates from the dye–oligonucleotide conjugates using reverse-phase chromatography, gel filtration chromatography, agarose, and acrylamide gel purification. In each case, the purification produced probes with lower quenching efficiencies, indicating that the link between the DNA and the gold is not completely stable.

**Table 2.** Comparison of the quenching efficiency of gold nanoparticles and DABCYL<sup>a</sup>

Dye	QE (%) of DABCYL- quenched beacons		QE (%) of gold-quenched beacons
	High-salt buffer	Low-salt buffer	
Fluorescein	98.59	96.55	99.42 ± 0.02
Rhodamine 6G	97.67	93.33	99.97 ± 0.03
Texas red	96.30	93.33	98.54 ± 0.04
Cy5	96.30	94.12	98.44 ± 0.03

<sup>a</sup>Comparison of the quenching efficiency (QE) of DABCYL-quenched beacons measured in high-salt buffer (1 M NaCl, 10 mM cacodylic acid, 0.5 mM EDTA, pH 7.3) and in low-salt buffer (90 mM KCl, 10 mM Tris, pH 8.0), with the quenching efficiency of the gold-quenched beacons. In both cases, only the best quenching efficiencies are reported. The standard errors are on the order of 0.05% for the DABCYL-quenched beacons.

Possible aggregation of the gold nanoparticles was investigated using fluorescence correlation spectroscopy<sup>14</sup>. We found that the diffusion constants of the DABCYL-quenched beacons and the gold-quenched beacons as they were hybridized to target 1 (refer to Fig. 1B) were very similar, indicating that the gold nanoparticles do not aggregate under our experimental conditions.

**Single-mismatch detection.** To separate matched from mismatched targets, the common procedure<sup>15</sup> is to work at a temperature at which hybridization to a matched probe is stable and to a mismatched one is unstable<sup>13</sup>. The usual temperature range used, between 50°C and 60°C, is not optimal for the quenching of the dye, because its average distance from the quencher increases with temperature. An alternative approach to distinguish between matched and mismatched targets is to work at room temperature and to use buffers with low salt concentrations. Because gold nanoparticles are unstable above 50°C, the latter approach was used in our experiments. In low-salt buffers, the quenching efficiency of the DABCYL beacons decreases (Table 2), but that of the gold-quenched beacon remains the same. This additional stability probably results from interactions between the dye and the gold cluster.

Screening of several buffers demonstrated that a buffer containing 90 mM KCl and 10 mM Tris, pH 8.0, gave the best sensitivity to mismatch detection; this buffer was subsequently used for all measurements. We studied the same probe sequence as before (Fig. 1B) and compared its hybridization to (1) a perfect target, 5'-GAAAAAAAAAAAAAAAA-3', which is complementary to the loop and to one base of the stem of the probe, and to (2) the same target with one mismatch, 5'-GAAAAAACAAAAAAAA-3'. Hybridization was tested for both targets at a wide range of concentrations (67 pM to 13 μM) in a solution containing 5 nM probe and 5 μM of a random pool of oligonucleotide sequences (Fig. 1B, target 4). The random sequences are used to test the specificity of the molecular beacons.

Two probes were used: a rhodamine–DNA–gold conjugate (Fig. 4A) and a rhodamine–DNA–DABCYL molecular beacon (Fig. 4B). We checked that the fluorescence of both probes is stable in the presence of 5 μM of random sequences (inset of Fig. 4A and 4B). This confirms the very high specificity of the molecular beacons.

Using either of the two probes, we were able to distinguish between the perfect target and the mismatch one, but the mismatch detection sensitivity differs significantly. If  $I_p(c)$  (or  $I_m(c)$ ) is the absolute fluorescence intensity when the concentration  $c$  of perfect (or mismatch) targets is present in solution, then the ratio  $I_p(c)/I_m(c)$  (see Fig. 4C) gives the sensitivity to the perfect target compared to the mismatched target when both are present in equimolar concentrations. For both probes, the best mismatch sensitivity is achieved around  $c_0 = 0.2 \mu\text{M}$  (Fig. 4C). At this concentration  $I_p/I_m$  is 25 for the dye–DNA–gold probe, whereas  $I_p/I_m$  is 4 for the molecular beacon.

**Competition between coexisting targets.** In the case of a mixed solution containing perfect, mismatched, and random targets, it is important to distinguish the perfect targets from the others<sup>22</sup>. The resolution  $R$  of the DNA probe is defined as the ratio between  $f(c_p, c_m, c_n)$  (i.e., the fluorescence of a solution of matched, mismatched, and random targets at the respective concentrations  $c_p, c_m, c_n$ ) and  $f(0, c_m, c_n)$ , the fluorescence of a solution of mismatched and random targets only:  $R = f(c_p, c_m, c_n)/f(0, c_m, c_n)$ .

The strategy is to fix the concentration of perfect targets to  $c_0$ , the optimum concentration for mismatch detection, and to change the concentration of mismatched targets,  $c_m$ . Because the random sequences do not bind to the probe (insets of Fig. 4A and B), the optimal  $R$  is a function of one parameter:  $c_m$ .  $R = f(c_0, c_m)/f(0, c_m)$

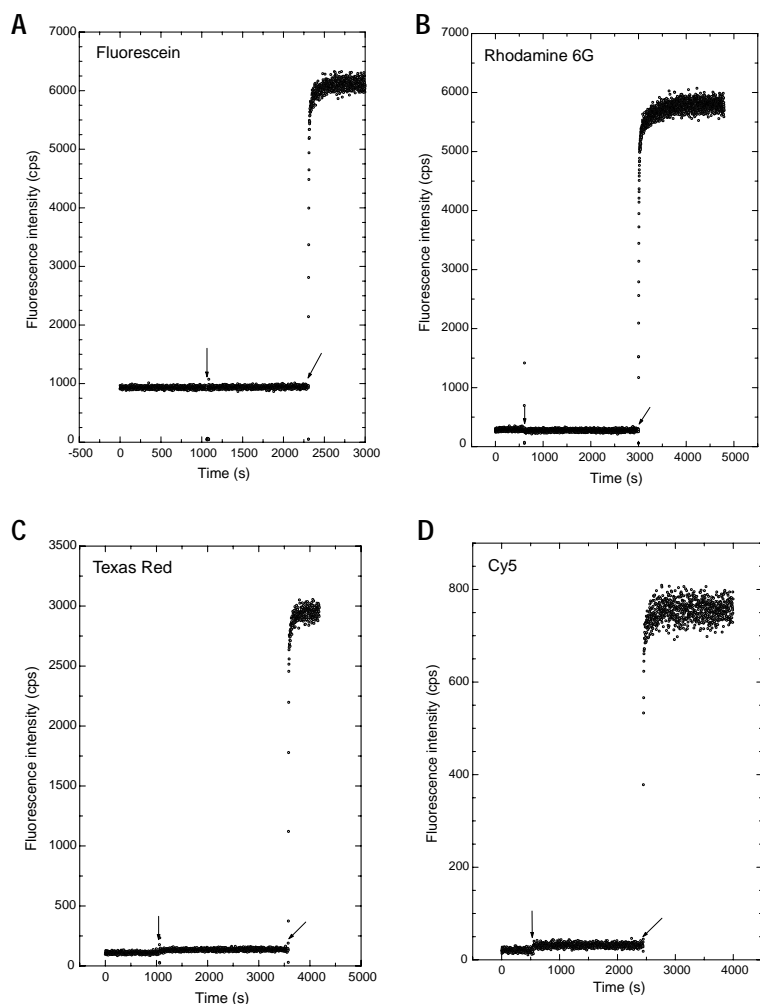


**Figure 3.** Efficiency of the quenching of gold nanoparticles. The emission spectrum of hairpin DNA coupled to gold and to (A) fluorescein, (B) rhodamine 6G, (C) Texas red, and (D) Cy5. For each spectrum, we distinguish three steps: (1) the cuvet is filled with buffer; (2) the dye–DNA–gold conjugates are introduced in the cuvet; (3) a 10-fold excess of target 1 is added. The transition between each regime is marked with an arrow. The oligonucleotide concentrations are 3 nM for fluorescein, 1.5 nM for Cy5, 3 nM for rhodamine 6G, and 5 nM for Texas red. The concentrations of gold present in each cuvet are 0.5  $\mu$ M for fluorescein, 0.4  $\mu$ M for Cy5, 0.5  $\mu$ M for rhodamine 6G, and 1  $\mu$ M for Texas red. The precise values of the fluorescence intensities for each dye and for each regime are reported in Table 1.

trum of the small 1.4 nm diameter gold particle we used decreases monotonically with increasing wavelength. No sign of surface plasmon resonance at the surface of the cluster is thus visible. For larger particles (diameter >3 nm), the absorption spectrum increases in intensity and shows a local maximum (at 520 nm for gold) characteristic of surface plasmon resonance<sup>26</sup>. At this particular wavelength, there is an additional decay channel for nonradiative energy transfer to the metal, and the quenching of fluorescence is optimal. The intensity, the position, and the number of the surface plasmon resonances of a metal cluster can be tuned precisely by changing the shape, the size, or the composition of the cluster<sup>27</sup>, so that the quenching can be optimized to a specific wavelength. It should be possible to optimize gold quenchers for each dye and use the differently colored gold-quenched beacons for simultaneous quantitation of multiple sequences.

The quenching ability of gold is not limited to its use in clusters. We anticipate that arrays of hairpin oligonucleotide–dye complexes can be attached on a gold surface and use the surface as a quencher of fluorescence. Coupling of fluorescence detection and surface plasmon resonance, a tool already widely used to detect molecular binding<sup>28</sup>, should provide extra sensitivity for oligonucleotide detection.

We showed that a hybrid material composed of a ssDNA covalently linked at each end to a gold nanoparticle and to an organic dye could be used as a molecular beacon with a quenching efficiency of  $99.966 \pm 0.026$ .

This result proves that gold-quenched nucleic acid probes can be more sensitive than other probes currently available. With these probes a point mutation can be selectively detected in the presence of random sequences even if only 1 out of 50 sequences has one mutation. However, additional improvements in the stability of the link between DNA and the metal cluster are required, so that purification of the gold–oligonucleotide–dye conjugate is possible without any loss in the quenching efficiency. A better understanding of the role of the gold surface ligands in keeping the dye and the gold in close proximity would help to optimize the quenching efficiency of the gold.

### Experimental protocol

**Synthesis of gold–DNA–dye conjugate.** We purchased the 25-base-long oligonucleotide 5'-S-S-GCGAGTTTTTTTTTTTTTCTCGC-NH<sub>2</sub>-3', which contained a disulfide group ended by a trityl moiety at the 5' end and a primary amino group at the 3' end (Midland Certified Reagent Company, Midland, TX). The disulfide group is covalently linked to the 5'-phosphate via a (CH<sub>2</sub>)<sub>6</sub> spacer, and the primary amino group is linked to the 3'-hydroxyl via a (CH<sub>2</sub>)<sub>7</sub> spacer. The oligonucleotide was purified with reverse-phase chromatography so as to select only the oligonucleotides that have the complete sequence and the necessary modifications.

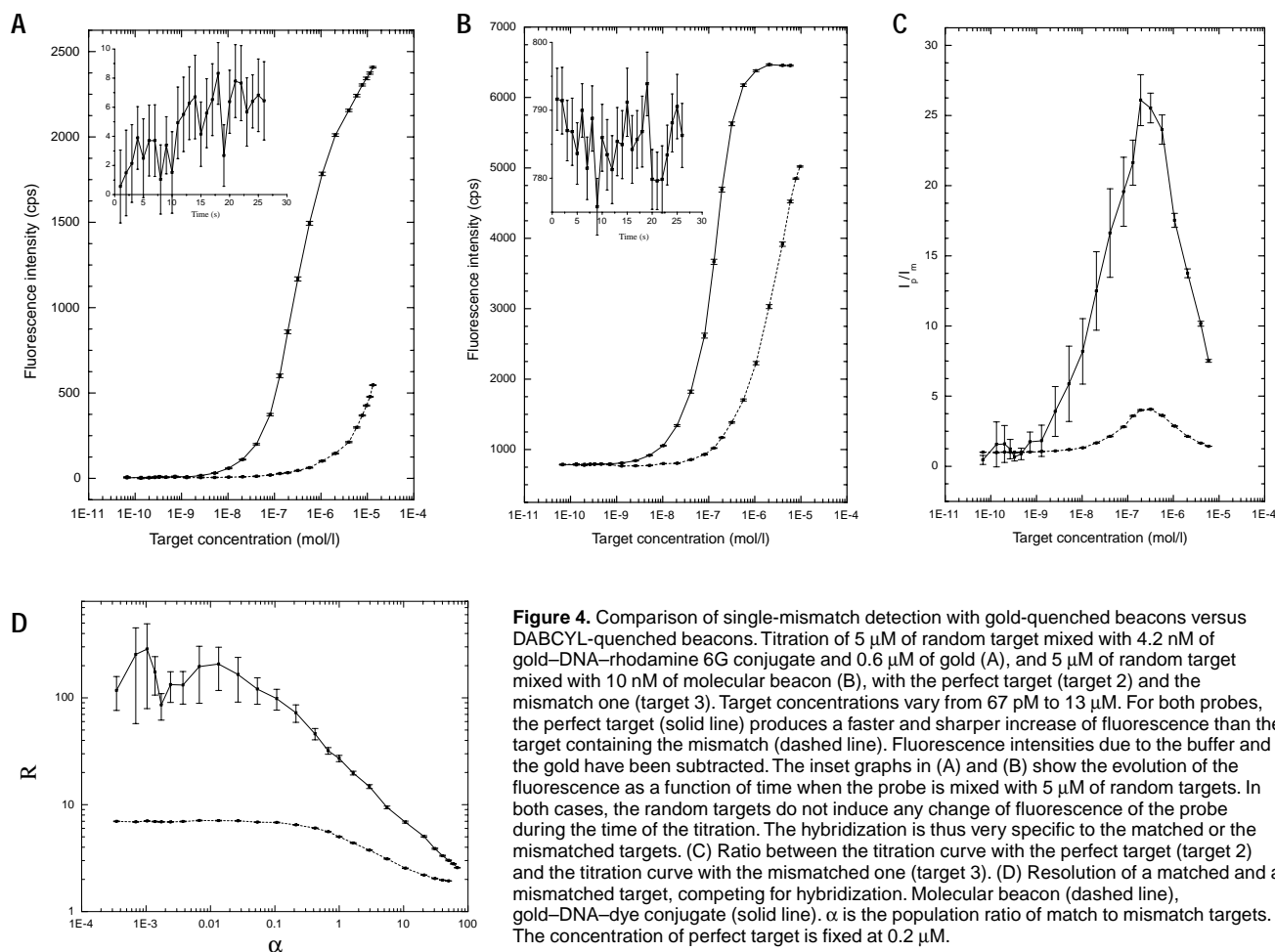
$= (I_p(c_0) + I_m(c_m)) / I_m(c_m)$  is presented in Figure 4D as a function of  $\alpha = c_0 / c_m$ .

The perfect target is detected when the fluorescence it produces is twice that due to the mismatched target alone, that is, when  $R$  is >3. This limit defines the resolution threshold. In the case of the molecular beacon,  $R$  is >3 for  $\alpha < 6$ , meaning that if 1 out of 6 DNA strands has the perfect sequence, it is detected, whereas for the hybrid probe,  $R$  is >3 for  $\alpha < 50$ , meaning that if 1 out of 50 DNA strands has the perfect sequence, it is detected. A greater than eightfold improvement is thus obtained with the hybrid probe.

### Discussion

The quenching of fluorescence by metals results primarily from non-radiative energy transfer from the dye to the metal<sup>23</sup>. Other types of quenching<sup>24</sup>, such as collisions of the dye against the gold surface (collisional or dynamic quenching) or interaction with the surface ligands of the gold cluster, may add to the quenching by the metal in our experiments. To test these possibilities, we replaced the 1.4 nm gold cluster with a 0.8 nm gold cluster (Undecagold), which has the same surface ligands and active group. No quenching was observed, indicating that the quenching observed with Nanogold is due primarily to the metal.

To our knowledge it has not been demonstrated previously that metal clusters may be used as efficient quenchers of fluorescence in biology. Our results open up interesting possibilities. The optical properties of metal clusters can be drastically altered through change of size, composition, shape, or type of surface ligands<sup>25</sup>. The absorption spec-



We then carried out two consecutive reactions. First, we covalently linked the amino-reactive dyes (fluorescein, rhodamine 6G, and Texas red (Molecular Probes, Eugene, OR) or Cy5 (Amersham Pharmacia Biotech, Piscataway, NJ)) to the 3'-amino group. We then covalently linked monomaleimido-gold particles (Nanoprobes, Yaphank, NY) to the 5'-sulfhydryl group. In the first coupling reaction, a 100  $\mu\text{l}$  solution containing 100  $\mu\text{M}$  oligonucleotide dissolved in 0.1 M sodium bicarbonate was reacted with 0.1 mg of a succinimidyl ester of the dye dissolved in 100  $\mu\text{l}$  of dimethyl sulfoxide. The reaction mixture was stirred at room temperature for 2 h. The reaction product was first purified with a Sephadex column (NAP-5; Amersham Pharmacia Biotech) equilibrated with 10 ml of 0.1 M triethylammonium acetate (pH 6.5). It was then fractionated on a  $\text{C}_{18}$  reverse-phase column (Bio-Rad Laboratories, Hercules, CA) with a linear elution gradient of 0 to 75% acetonitrile dissolved in 0.1 M triethylammonium acetate (pH 6.5) at a flow rate of 1 ml/min. The fractions that absorbed at 260 nm and at the dye maximum absorption were isolated. The fractions collected were partially dried in a SpeedVac (Savant, Farmingdale, NY) and purified again using a Sephadex column equilibrated with 0.1 M sodium bicarbonate (pH 8.3). The elution volume was concentrated with Ultrafree-0.5 centrifuge columns with a  $M_r$  5,000 cutoff (Millipore, Bedford, MA) to a final oligonucleotide concentration of 15  $\mu\text{M}$ . The disulfide bond was cleaved with dithiothreitol (DTT), and the oligonucleotide was purified of excess DTT before coupling to the gold. Then, 10  $\mu\text{l}$  of 1 M DTT were added to 25  $\mu\text{l}$  of oligonucleotide mixed with 75  $\mu\text{l}$  of sodium bicarbonate, pH 8.3. After a 1 h incubation, the oligonucleotide solution was purified using reverse-phase chromatography, as described. The fractions containing the activated oligonucleotide were purified using a Sephadex column (NAP-5) equilibrated with water. Part of the elution product (37 pmol to 370 pmol of DNA, suspended in 180  $\mu\text{l}$  of water) was immediately reacted with 6 nmol of the monomaleimido-gold particles (Nanoprobes) in aqueous 20 mM  $\text{NaH}_2\text{PO}_4$ , 150 mM NaCl, 1 mM ethylenediamine tetraethyl acetate (EDTA) buffer, pH 6.5, containing 10%

isopropanol at 4°C for 24 h. Reaction products were analyzed by gel electrophoresis on a 10% nondenaturing acrylamide gel performed in 1 $\times$  Tris-borate EDTA (TBE) at 10 V/cm.

**Measure of the gold quenching efficiency.** The quenching efficiency ( $QE$ ) of the gold-oligonucleotide-dye is defined as  $100 \times (1 - (i_{\text{closed}}/i_{\text{open}}))$ , where  $i_{\text{closed}}$  is the fluorescence intensity of a molecular beacon in the absence of target, and  $i_{\text{open}}$  is its fluorescence when bound to target. It is computed from the experimental intensities as  $100 \times (I_{\text{iv}} - I_{\text{ii}})/(I_{\text{iv}} - I_{\text{iii}})$  (see Table 1). Here,  $I_{\text{iv}} = i_{\text{open}} + I_{\text{iii}}$  and  $I_{\text{ii}} = i_{\text{closed}} + I_{\text{iii}}$ .

Fluorescent measurements were performed on a spectrofluorometer (Photon Technology International, Monmouth Junction, NJ) using a 10 mm pathlength quartz cuvet (NSG Precision Cells, Farmingdale, NY) with temperature fixed at 20°C with a circulating waterbath. The background fluorescence of 3 ml of the buffer containing 1 M NaCl, 10 mM cacodylic acid, 0.5 mM EDTA (pH 7.3) was monitored for a few minutes. Then, 10 to 100  $\mu\text{l}$  of the mixture of uncoupled gold and gold-DNA-dye conjugate was added to the hybridization buffer and fluorescence was measured. After confirming that there was no change of fluorescence with time, an excess of target oligonucleotide (5'-AAAAAAAAAAAAAAAACTCGC-3') was added, and the level of fluorescence was recorded. This experiment was repeated with four different dyes. For each dye, the excitation and the emission wavelengths of the fluorometer were adjusted to match those given by the manufacturer: (494 nm; 520 nm) for fluorescein (524 nm; 557 nm) for rhodamine 6G (583 nm; 603 nm) for Texas red, and (649 nm; 670 nm) for Cy5. The change in the fluorescence level due to the gold particles alone was measured at the wavelengths used for each dye. From 1.2 to 3 nmol of pure Nanogold particles were suspended under the same conditions as the gold used for coupling to the oligonucleotide. The change of fluorescence background was measured as the gold was added to the hybridization buffer.

The molecular beacons were synthesized by reacting a succinimidyl ester



## RESEARCH ARTICLE

dye to the primary amine located at the 5' end of an oligonucleotide (5'-NH<sub>2</sub>-GCGAGTTTTTTTTTTTTTCTCGC-3'-DABCYL) that had a DABCYL covalently linked at its 3' end.

**Mismatch detection.** For the mismatch detection, the hybridization buffer was composed of 90 mM KCl, 10 mM Tris, pH 8.0. We successively tested the detection of one mismatch in a sequence of 16 bases with two probes having the same oligonucleotide sequence and the same dye (rhodamine 6G) with either Nanogold or DABCYL as the quencher. A 180  $\mu$ l aliquot of a solution containing 37 pmol of oligonucleotide and 4.8 nmol of monomaleimido-gold particles was equally divided in three vials (1–3), each containing 60  $\mu$ l of the product. The contents of vial 1 were mixed with 3 ml of the hybridization buffer and after a few minutes with 100  $\mu$ l of 160  $\mu$ M of target 4 (Fig. 1B). This pool of oligonucleotides acts as random targets competing with the perfect and the mismatched targets. We checked that the level of fluorescence did not change over 30 min. The same procedure was repeated with vial 2, but immediately after the addition of the random sequences,

perfect targets (5'-GAAAAAAAAAAAAAAAA-3') were added in steps 1 min apart. The target concentration gradually increased from 67 pM to 13  $\mu$ M. The same titration was repeated with vial 3 but with a target containing one mismatch (5'-GAAAAAAAAA C AAAAAAAAA-3'). Each target was suspended in the hybridization buffer so that the composition of the buffer did not change during the titration. A titration experiment typically lasted 30 min. Similar titrations were done with the probe that had the DABCYL as the quencher.

**Acknowledgments**

We thank G. Bonnet for enlightening discussions and suggestions, and for his help with the fluorescence correlation spectroscopy measurements. We thank R. Bar-Ziv, G. V. Shivashankar, T. Tomoda, and A. Mehta for interesting discussions. The help of A. Roll-Mecak and D. Stettler was instrumental in the final writing of this manuscript. We also thank the reviewers for improvement to the manuscript. This research was supported by the Mathers Foundation.

Received 27 June 2000; accepted 12 December 2000

- Mirkin, C.A., Letsinger, R.L., Mucic, R.C. & Storhoff, J.J. A DNA-based method for rationally assembling nanoparticles into macroscopic materials. *Nature* **382**, 607–609 (1996).
- Alivisatos, A.P. *et al.* Organization of nanocrystal molecules using DNA. *Nature* **382**, 609–611 (1996).
- Mitchell, G.P., Mirkin, C.A. & Letsinger, R.L. Programmed assembly of DNA functionalized quantum dots. *J. Am. Chem. Soc.* **121**, 8122–8123 (1999).
- Whaley, S.R., English, D.S., Hu, E.L., Barbara, P.F. & Belcher, A.M. Selection of peptides with semiconductor binding specificity for directed nanocrystal assembly. *Nature* **405**, 665–668 (2000).
- Schultz, S., Smith, D.R., Mock, J.J. & Schultz, D.A. Single-target molecule detection with nonbleaching multicolor optical immunolabels. *Proc. Natl. Acad. Sci. USA* **97**, 996–1001 (2000).
- Elghanian, R., Storhoff, J.J., Mucic, R.C., Letsinger, R.L. & Mirkin, C.A. Selective colorimetric detection of polynucleotides based on the distance-dependent optical properties of gold nanoparticles. *Science* **277**, 1078–1081 (1997).
- Storhoff, J.J., Elghanian, R., Mucic, R.C., Mirkin, C.A. & Letsinger, R.L. One-pot colorimetric differentiation of polynucleotides with single base imperfections using gold nanoparticle probes. *J. Am. Chem. Soc.* **120**, 1959–1964 (1998).
- Andrew, T.A., Mirkin, C.A. & Letsinger, R.L. Scanometric DNA array detection with nanoparticle probes. *Science* **289**, 1757–1760 (2000).
- Loweth, C.J., Caldwell, W.B., Peng, X.G., Alivisatos, A.P. & Schultz, P.G. DNA-based assembly of gold nanocrystals. *Angew. Chem. Int. Edn. Engl.* **38**, 1808–1812 (1999).
- Niemeyer, C.M., Burger, W. & Peplies, J. Covalent DNA–Streptavidin conjugates as building blocks for novel biometallic nanostructures. *Angew. Chem. Int. Edn. Engl.* **37**, 2265–2268 (1998).
- Storhoff, J.J. *et al.* What controls the optical properties of DNA-linked gold nanoparticle assemblies? *J. Am. Chem. Soc.* **122**, 4640–4650 (2000).
- Tyagi, S. & Kramer, F.R. Molecular beacons: probes that fluoresce upon hybridization. *Nat. Biotechnol.* **14**, 303–308 (1996).
- Bonnet, G., Tyagi, S., Libchaber, A. & Kramer, F.R. Thermodynamic basis of the enhancement specificity of structured DNA probes. *Proc. Natl. Acad. Sci. USA* **96**, 6171–6176 (1999).
- Bonnet, G., Krichevsky, O., & Libchaber, A. Kinetics of conformational fluctuations in DNA hairpin-loops. *Proc. Natl. Acad. Sci. USA* **95**, 8602–8606 (1998).
- Marras, S.A.E., Kramer, F.R. & Tyagi, S. Multiplex detection of single-nucleotide variations using molecular beacons. *Genet. Anal.-Biomol. E.* **14**, 151–156 (1999).
- Stemmers, F.J., Ferguson, J.A. & Walt, D.R. Screening unlabeled DNA targets with randomly ordered fiber-optic gene array. *Nat. Biotechnol.* **18**, 91–94 (2000).
- Tyagi, S., Bratu, D.P. & Kramer, F.R. Multicolor molecular beacons for allele discrimination. *Nat. Biotechnol.* **16**, 49–53 (1997).
- Vet, J.A.M. *et al.* Multiplex detection of four pathogenic retroviruses using molecular beacons. *Proc. Natl. Acad. Sci. USA* **96**, 6394–6399 (1999).
- Gersten, J. & Nitzan, A. Spectroscopic properties of molecules interacting with small dielectric particles. *J. Chem. Phys.* **75**, 1139–1152 (1981).
- Weitz, D.A., Garoff, S., Gersten, J.I. & Nitzan, A. The enhancement of Raman scattering, resonance Raman scattering, and fluorescence from molecules adsorbed on a rough silver surface. *J. Chem. Phys.* **78**, 5324–5338 (1983).
- Moskovits, M. Surface-enhanced spectroscopy. *Rev. Mod. Phys.* **57**, 783–826 (1985).
- Bonnet, G. & Libchaber, A. Optimal sensitivity in molecular recognition. *Physica A* **263**, 68–77 (1999).
- Chance, R.R., Prock, A. & Silbey, R. Molecular fluorescence and energy transfer near interfaces. *Adv. Chem. Phys.* **37**, 1–65 (1978).
- Lakowicz, J.R. *Principles of fluorescence spectroscopy*, Edn 2. (Kluwer Academic, New York; 1999).
- Kreibig, U. & Vollmer, M. *Optical properties of metal clusters*. (Springer-Verlag, Berlin; 1995).
- Doremus, R.H. Optical properties of small gold particles. *J. Chem. Phys.* **40**, 2389–2396 (1964).
- Chang, S.-S., Shih, C.-W., Chen, C.-D., Lai, W.-C. & Chris Wang, C.R. The shape transition of gold nanorods. *Langmuir* **15**, 701–709 (1999).
- Lyon L.A. *et al.* Raman spectroscopy. *Anal. Chem.* **70**, 341R–361R (1998).
- Hainfeld, J.F. Undecagold-antibody method. In *Colloidal gold: principles, methods and applications*, Vol. 2. (ed. Hayat, M.A.) 413–429 (Academic Press, San Diego, CA; 1989).